

New fission-track results from the northern Chiapas Massif area, SE Mexico: trying to reconstruct its complex thermo-tectonic history

Fanis Abdullin^{1,*}, Luigi Solari¹, Carlos Ortega-Obregón¹, and Jesús Solé²

¹Centro de Geociencias, Universidad Nacional Autónoma de México, Blvd. Juriquilla No. 3001, Querétaro, 76230, Mexico.

²Instituto de Geología, Universidad Nacional Autónoma de México, Ciudad Universitaria, 04510, Ciudad de México, Mexico.

*fanisius@yandex.ru

ABSTRACT

The Chiapas Massif Complex, which represents the crystalline basement of the southern Maya block within the North American plate, records numerous thermo-tectonic and magmatic events that occurred in southern Mexico at least since the late Mesoproterozoic. The present study was performed across the northern Chiapas Massif region to reconstruct its complex thermo-tectonic history from Mesozoic to present times. Basement samples and sandstones of the San Ricardo Formation derived from the Chiapas Massif Complex source area were analyzed by *in situ* apatite fission-track dating. The new fission-track results obtained in this study, together with previously published data, indicate that the Chiapas Massif Complex, or rather the whole Maya terrane, have experienced a complex long-term geodynamic evolution with at least five post-Permian tectonic and magmatic events: (1) a Late Triassic cooling event, likely related to the initial breakup of Pangea; (2) Early Jurassic volcanism that can be linked to the Nazas volcanic arc; (3) a Middle Jurassic tectonic event that was triggered by continental rifting at the beginning of the opening of the Gulf of Mexico; (4) a Late Cretaceous to Paleocene orogeny that may actually represent the southernmost continuation of the Laramide *sensu lato* which affected central and northern Mexico; and (5) the middle-late Miocene Chiapanecan event that is tectonically controlled by the interaction of the North American, Caribbean, and Cocos plates. This interpretation could be useful towards a better understanding of the geological history of southern North America. Some recommendations on sampling and analytical strategies are also given for consideration in further thermochronological studies in Chiapas.

Key words: thermochronology; tectonic evolution; magmatism; Chiapas Massif; Chortís block; Mexico.

RESUMEN

El Macizo de Chiapas, el cual representa al basamento cristalino de la parte sur del bloque Maya dentro de la placa Norteamericana, conserva abundantes señales de eventos tectono-térmicos y magmáticos que ocurrieron en el sur de México desde el Mesoproterozoico tardío. El

*presente estudio se realizó en el área norte del Macizo de Chiapas con el objetivo general de reconstruir su compleja historia tectono-térmica para el periodo desde el Mesozoico hasta el presente. Muestras del basamento y areniscas de la Formación San Ricardo que procedieron del Macizo de Chiapas fueron analizadas por la técnica de trazas de fisión *in situ* en apatitos. Las nuevas edades por trazas de fisión en apatitos, así como algunos resultados previamente publicados, indican que el Macizo de Chiapas y todo el Terreno Maya han experimentado una historia geodinámica muy compleja que abarca un mínimo de cinco eventos tectónicos y magnéticos post-pérmicos: (1) un evento de enfriamiento en el Triásico Tardío, posiblemente relacionado con la ruptura inicial de Pangea; (2) volcanismo del Jurásico Temprano que puede asociarse al arco volcánico Nazas; (3) un evento tectónico del Jurásico Medio, muy probablemente activado por rifting continental durante el comienzo de la apertura del Golfo de México; (4) una orogénesis del Cretácico Tardío al Paleoceno que puede representar la continuación más austral de la orogenia Laramide sensu lato que afectó el centro y norte de México; y (5) un evento orogénico del Mioceno medio-tardío conocido como el evento Chiapaneco, el cual está controlado por la interacción de las placas tectónicas Norteamericana, Caribe y Cocos. Estas interpretaciones podrían ser útiles para entender mejor la historia geodinámica de la parte sur de Norteamérica. Se sugieren algunas estrategias de muestreo y analíticas para futuros estudios termocronológicos en Chiapas.*

Palabras clave: termocronología; evolución tectónica; magmatismo; Macizo de Chiapas; Bloque Chortís; México.

INTRODUCTION

The area of Chiapas, geodynamically controlled by the interaction of the North American, Caribbean, and Cocos plates (Guzmán-Speziale *et al.*, 1989; Meneses-Rocha, 2001; Authemayou *et al.*, 2011; Witt *et al.*, 2012; Molina-Garza *et al.*, 2015), can be considered as a complex geological province of southern Mexico. The Chiapas Massif Complex (CMC) is the “root” of an active continental margin formed during the late Permian to Triassic and actually represents the crystalline basement of the southern Maya block within the North American plate (Figure 1), as it was interpreted by several authors (e.g., Dengo, 1985; Meneses-Rocha, 1985, 2001; Schaaf *et al.*, 2002; Weber *et al.*, 2005,

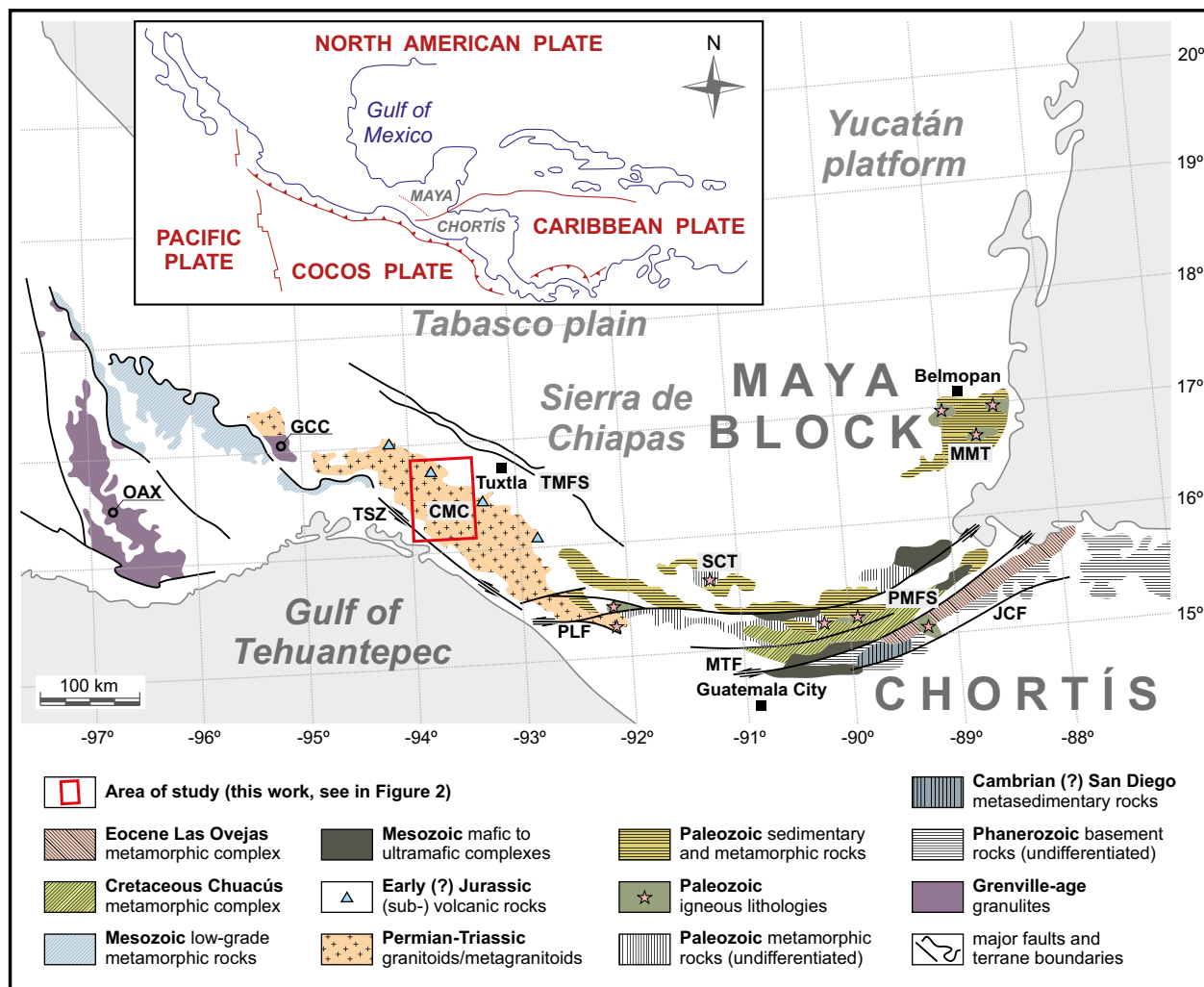


Figure 1. Regional geodynamic setting of southern Mesoamerica and simplified geologic map of southern Mexico (modified from Martínez-Amador *et al.*, 2005; Weber *et al.*, 2008; Estrada-Carmona *et al.*, 2012; Torres-de León *et al.*, 2012; Solari *et al.*, 2013; Cisneros de León *et al.*, 2017). CMC—Chiapas Massif Complex; GCC—Guichicovi Complex; JCF—Jocotán-Chamelecón fault; MMT—Maya Mountains; MTF—Motagua fault; OAX—Oaxacan Complex; SCT—Sierra de los Cuchumatanes; PLF—Polochic fault; PMFS—Polochic-Motagua Fault System; TMFS—Tuxtla-Malpaso Fault System; TSZ—Tonala Shear Zone.

2007). Numerous field observations, petrogenetic, as well as high- to medium-temperature geochronological studies were performed in the CMC to understand its origin and to reconstruct its geological history for Paleozoic to early Mesozoic times (Damon *et al.*, 1981; Torres *et al.*, 1999; Schaaf *et al.*, 2002; Weber *et al.*, 2005, 2006, 2007, 2008, 2009; Estrada-Carmona *et al.*, 2009, 2012; Pompa-Mera, 2009; González-Guzmán *et al.*, 2016). Recent studies by González-Guzmán *et al.* (2016) and Cisneros de León *et al.* (2017) indicate that the geodynamic evolution of the CMC, as well as of the whole Maya block, started, at least, in the late Mesoproterozoic. The CMC, therefore, may include abundant signals (e.g., crystallization or cooling ages) of either thermo-tectonic or magmatic events that occurred in southern Mexico, which can be used to better reconstruct the tectonic history of southern North America.

Despite of its strategic locality (*i.e.*, in southern Maya block and very close to the Chortis block; Figure 1), no detailed and systematic low-temperature thermochronological studies have been carried out in the CMC to detect relatively younger tectonic events that occurred from Mesozoic to present. Such studies, including primarily apatite fission-track (AFT) and zircon fission-track analyses and helium dating, are

particularly useful to understand the evolution of the uppermost continental crust that may be controlled by rifting, collisional, diagenetic, low- to medium-grade metamorphic, hydrothermal, or denudation processes, *among others* (e.g., Ehlers and Farley, 2003; Reiners *et al.*, 2005; Reiners and Brandon, 2006; Mark *et al.*, 2014). A few AFT results from the central CMC, ranging from ~40 to ~25 Ma (Ratschbacher *et al.*, 2009), were interpreted as indicating a rapid cooling of the CMC in the Oligocene (more than 2 km of exhumation and erosion at $\sim 30 \pm 3$ Ma), a cooling signal that could have been triggered by the hypothetical arrival of the Chortis block in front of the Gulf of Tehuantepec (e.g., Ratschbacher *et al.*, 2009; Witt *et al.*, 2012). Other AFT results, reported by Witt *et al.* (2012), apparently dismiss the possibility of a rapid cooling of the CMC during the Oligocene. AFT analysis-derived time-temperature modeling for two sandstones sampled from the Middle(?) Jurassic Todos Santos Formation in the northern CMC area, as well as provenance studies performed in some Cenozoic units from the Sierra de Chiapas (including studies of Witt *et al.*, 2012) suggest that in the CMC not only the Oligocene, but most of the Cenozoic was a tectonically quiescent period (approximately from Eocene to middle Miocene; Abdullin *et al.*, 2016a, 2016b).

Thus, up to now, somewhat controversial interpretations about the Cenozoic evolution of the CMC are proposed in these pioneering thermochronological studies. The Cenozoic tectonics of the CMC is of a particular interest because many authors (e.g., Schaaf *et al.*, 1995; Pindell *et al.*, 2006; Ratschbacher *et al.*, 2009; Torres-de León *et al.*, 2012; Witt *et al.*, 2012) suggested an Oligocene arrival of the Chortíz block to the Gulf of Tehuantepec region (*i.e.*, as a collision of the Chortíz and Maya continental blocks), which should have been imprinted in the tectonic history of the CMC as a rapid cooling period as well as by ubiquitous stratigraphic records within Oligocene units from the inner parts of the Sierra de Chiapas (e.g., the presence of granitic conglomerates derived from the CMC rocks). Despite the controversy surrounding the Oligocene thermal history, all these AFT data detected a middle to late Miocene thermo-tectonic event that affected almost the entire territory of Chiapas (Ratschbacher *et al.*, 2009; Witt *et al.*, 2012; Abdullin *et al.*, 2016a), which is essentially well-known as the Chiapanecan orogeny (e.g., Sánchez-Montes de Oca, 1979, 2006; Meneses-Rocha, 2001; Padilla y Sánchez, 2007; Guzmán-Speziale, 2010). A Late Cretaceous to late Paleocene–early Eocene orogenic event was proposed previously for Chiapas by several authors (Gutiérrez-

Gil, 1956; Sánchez-Montes de Oca, 1979, 2006; Carfantán, 1981, 1985; Moravec, 1983; Meneses-Rocha, 1985, 1991, 2001), a hypothesis that seems to be confirmed by recent AFT analyses performed by Abdullin *et al.* (2016a).

In this work, new AFT ages are reported and a brief review of the stratigraphy of Chiapas is presented as well, with the purpose to reconstruct the complex tectonic evolution of the Chiapas Massif Complex from Mesozoic to present times. To extract ages of tectonic or magmatic events that occurred during the geological history of the CMC, basement rocks of the CMC and Mesozoic sandstones from the Oxfordian to Aptian San Ricardo Formation were analyzed by *in situ* AFT technique.

STUDY AREA

The present study is focused on the north-central part of the CMC region (Figure 1). The study area displays large exposures of the CMC (Figure 2; basement rocks are not differentiated in the map). The CMC predominantly includes late Permian–Triassic calc-alkaline interme-

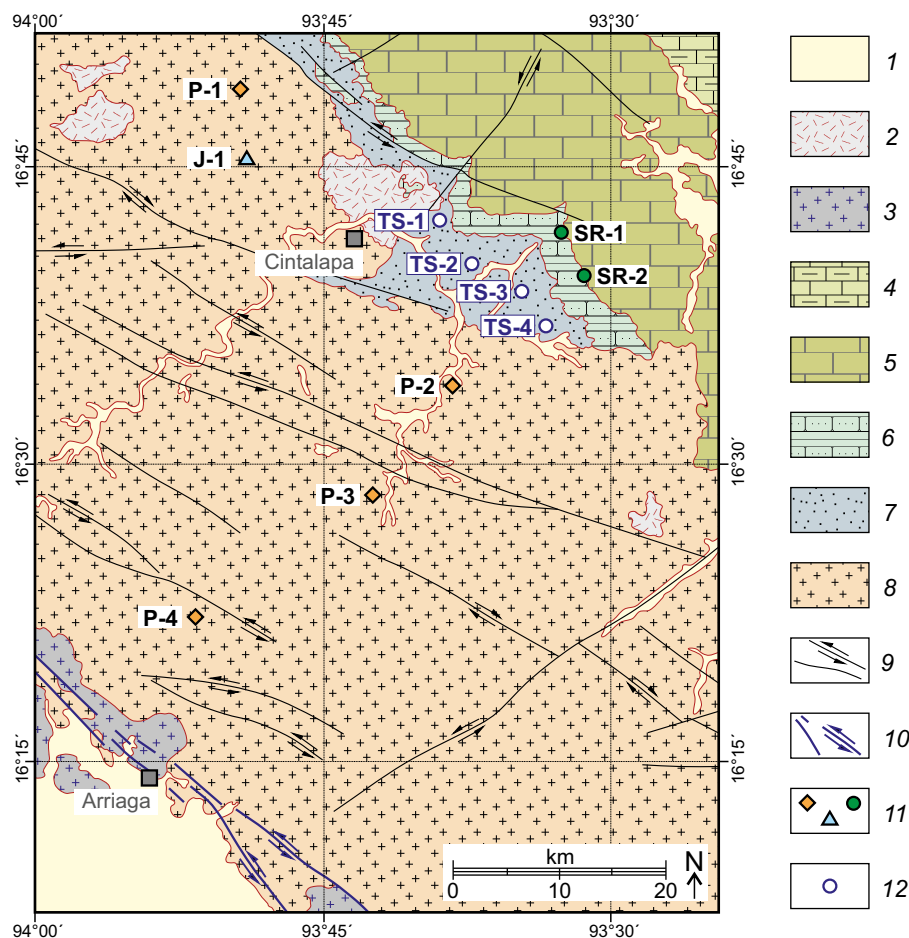


Figure 2. Simplified geological map of the northern Chiapas Massif area (modified after Martínez-Amador *et al.*, 2005; Weber *et al.*, 2008; Molina-Garza *et al.*, 2015) showing the location of sampling sites for *in situ* AFT analysis. 1 – Quaternary sediments; 2 – Miocene volcanic and volcanoclastic lithologies; 3 – Miocene granites; 4 – Campanian to Maastrichtian Ocozocoautla Formation (gravel to marly sandstones, shales with marls, and limestones); 5 – Albian–Santonian Sierra Madre Formation (limestones and dolomites); 6 – Oxfordian to Aptian San Ricardo Formation (carbonates, marls, shales, and sandstones); 7 – Late Triassic (?) to Oxfordian Todos Santos Formation (conglomerates, volcanoclastic sediments, and fine-grained to coarse-grained sandstones); 8 – Chiapas Massif Complex (undifferentiated, mostly includes late Permian–Early Triassic granitoids and metamorphic rocks); 9 – strike-slip faults; 10 – Tonalá Shear Zone; 11 – samples analyzed by *in situ* AFT technique (this study); 12 – sandstones from Todos Santos Formation that were analyzed previously by AFT thermochronology (Abdullin *et al.*, 2016a).

diate to felsic plutonic rocks, most of which are strongly deformed while others are metamorphosed (Damon *et al.*, 1981; Torres *et al.*, 1999; Schaaf *et al.*, 2002; Weber *et al.*, 2005, 2007; Estrada-Carmona *et al.*, 2009).

In this area, the base of the outcropping sedimentary cover is seemingly represented by red beds of the Todos Santos Formation (Figure 2), which unconformably overlies the CMC, and includes, from bottom to top, conglomerates, volcanoclastic materials, fine-grained, lacustrine and fluvial, medium- to coarse-grained (sub-) arkosic sandstones and conglomerates (Meneses-Rocha, 1985, 2001; Blair, 1987; Godínez-Urban *et al.*, 2011). Its variable thickness, from 250 m to 1,350 m, can be related to a graben-like geometry derived from extensional processes associated with continental rifting (Sánchez-Montes de Oca, 1979, 2006; Meneses-Rocha, 1985, 2001; Blair, 1987; Padilla y Sánchez, 2007; Godínez-Urban *et al.*, 2011). Because the Todos Santos Formation is continental, it is very difficult to determine its exact age. Nonetheless, most authors argue that these red beds were probably deposited in the Middle Jurassic (Quezada-Muñetón, 1983; Meneses-Rocha, 1985, 2001; Mandujano-Velásquez, 1996; Sánchez *et al.*, 2004; Sánchez-Montes de Oca, 2006; Godínez-Urban *et al.*, 2011; Abdullin *et al.*, 2016a, 2016b).

The San Ricardo Formation conformably overlies the Todos Santos Formation (Figure 2). It includes three members, Oxfordian to Kimmeridgian carbonates, Tithonian marls with shales, and Berriasian to Aptian fine-grained sandstones, and its total thickness varies from 500 to 1400 m (Quezada-Muñetón, 1983; Mandujano-Velásquez, 1996; Sánchez *et al.*, 2004). The lowermost beds were interpreted as a transgressive sequence above the Todos Santos Formation (Quezada-Muñetón, 1983; Meneses-Rocha, 2001; Sánchez-Montes de Oca, 2006). The Albian-Santonian Sierra Madre Formation (1,000–2,500 m thick) is mainly composed of limestones and dolomites deposited on a marine platform during a period of tectonic stability (e.g., Rosales-Domínguez *et al.*, 1997; Rosales-Domínguez, 1998). The 300 to 800 m-thick Campanian-Maastrichtian Ocozocoautla Formation, which was deposited in a shoreline setting, consists, from base to top, of gravel, coarse-grained to marly sandstones, alternating thin layers of shales and marls, and limestones (Mandujano-Velásquez, 1996; Rosales-Domínguez, 1998). The high-energy siliciclastic sediments at the base of this unit could announce the beginning of a Late Cretaceous–early Paleogene orogeny that destroyed some parts of the Albian to Santonian platform (e.g., Meneses-Rocha, 1985, 1991, 2001; Abdullin *et al.*, 2016a). The denudation of the westernmost areas of Chiapas during the Late Cretaceous–early Paleogene orogenic event is also well registered in the Campanian-Maastrichtian Méndez Formation and the Paleocene Soyaló, Lutitas Nanchital, and Conglomerado Uzpanapa formations, all of which contain abundant fragments of calcareous rocks derived from the Albian-Santonian carbonate platform (Meneses-Rocha, 1985; Quezada-Muñetón, 1987; Sánchez-Montes de Oca, 2006). Cenozoic sedimentary rocks were not recognized in the study area (Figure 2). The Cenozoic lithostratigraphic column of Chiapas is dominantly siliciclastic in composition with minor shallow water deposits locally associated with carbonate to mixed siliciclastic-carbonate platforms, all of which crop out in the central, northern, and eastern portions of the Sierra de Chiapas (Meneses-Rocha, 1985, 2001; Quezada-Muñetón, 1987; Sánchez *et al.*, 2004; Sánchez-Montes de Oca, 2006; Padilla y Sánchez, 2007; Witt *et al.*, 2012). During the middle to late Miocene, igneous activity took place along the CMC (e.g., Molina-Garza *et al.*, 2015) and generated ubiquitous intrusions along the Tonalá shear zone (Figure 1) in the SW as well as the emplacement of some volcanic rocks and volcanoclastic deposits in the NE (Figure 2).

To solve the objectives of the present study, a total of seven rocks were sampled: five basement samples from the CMC and two fine-grained sandstones from the Berriasian–Aptian sandy member of

the San Ricardo Formation (Figure 2). Basement rocks (P-1, P-2, P-3, P-4 and J-1) were collected principally to obtain relatively recent (*i.e.*, Cenozoic) AFT ages in the CMC. Based on LA-ICP-MS zircon chronology, P-1, P-2, P-3, and P-4 were identified as late Permian (Lopingian) igneous and metagranitic samples, whereas J-1 yielded a Sinemurian crystallization age of 196 ± 2 (2σ) Ma (Ortega-Obregón *et al.*, 2016). Two detrital samples were obtained from the San Ricardo Formation (SR-1 and SR-2). Due to the fact that they were mostly derived from the CMC and include apparently unreset apatites (Abdullin *et al.*, 2016b), those sediments can be very useful to indirectly detect any signals of older cooling events, which apparently took place within the CMC prior to the deposition of this unit. Coordinates of rock samples and other details may be consulted in the Supplementary Appendix A1.

ANALYTICAL PROCEDURES

Heavy minerals were concentrated from the two narrow grain-size fractions of 60–125 and 125–180 μm using conventional techniques like crushing, sieving, WilfleyTM table, and FrantzTM separator. Nearly 300 apatite grains, extracted from each sample under a binocular microscope, were mounted with EpoFixTM (Struers) in a 2.5-cm-diameter plastic ring, and then were sequentially polished with SiC MicroCutTM Buehler sandpaper P-1500 ($\sim 13 \mu\text{m}$) and P-2500 ($\sim 8 \mu\text{m}$) and alumina suspensions (3, 1, 0.3, and 0.1 μm) over MicroClothTM Buehler pads. Polished apatites were etched in 5.5 M HNO₃ at 21 °C for 20 s to reveal ²³⁸U spontaneous fission tracks (*i.e.*, radiation damages produced by expulsed “daughter nuclides”) generated by the natural fission of ²³⁸U atoms (“parent nuclides”), a chemical protocol commonly used in the sample preparation for AFT analyses (e.g., Wagner and Van den haute, 1992; Donelick *et al.*, 2005). Fission track counting and confined track and etch pit length measurements were performed using OlympusTM BX-51 and LeicaTM DM microscopes with “dry” objectives, both upgraded with high-resolution digital cameras and an image processing software. In the case of basement samples, only clear apatite crystals with homogeneously distributed tracks were selected for AFT dating, whereas apatite crystals from siliciclastic samples were selected randomly. Detrital apatite with many visible inclusions, which hinder adequate observation of tracks, as well as those with a strong track density zoning (with an evident zonation of U) were excluded from AFT dating, because these may yield highly biased single-grain AFT ages using the LA-ICP-MS-based technique (Hasebe and Arai, 2007; Abdullin *et al.*, 2014, 2016a; Liu *et al.*, 2014; Vermeesch, 2017). In some apatite grains, spontaneous track densities (ρ_s) values were obtained from small areas, $\sim 4,000$ to $\sim 5,500 \mu\text{m}^2$ (for single-spot micro-sampling by LA-ICP-MS), whereas in larger crystals track counting was performed within areas from $\sim 8,000$ to $\sim 18,000 \mu\text{m}^2$ (for multi-spot analyses; from two to four spots per grain). For most apatite samples dated, chlorine contents were measured simultaneously by LA-ICP-MS to calibrate annealing properties of fission tracks. Additionally, in some detrital apatites from the San Ricardo Formation, *D*-par proposed by Raymond Donelick was also used as a main kinetic parameter (*i.e.*, the mean etch pit length measured parallel to the crystallographic *C*-axis of apatite using reflected light on a polished and etched surface; see Donelick *et al.*, 2005).

Sample preparation was performed in the Taller de Molienda and Taller de Laminación, while optical studies and LA-ICP-MS analyses were carried out in the Laboratorio de Estudios Isotópicos (LEI Lab), all at Centro de Geociencias (CGEO), Universidad Nacional Autónoma de México (UNAM), Campus Juriquilla. The micro-sampling with LA-ICP-MS was carefully performed within the areas observed previously to determine the ρ_s values (for instance, see fig. 2 in Vermeesch, 2017

or fig. 3 of Abdullin *et al.*, 2016a). Raw data were reduced off-line using the Iolite™ 3.4 program (Paton *et al.*, 2011). The results for measured isotopes using the NIST612 glass (Pearce *et al.*, 1997) were normalized using ^{43}Ca as an internal standard and taking an average CaO content, according to Lesnov (2012), for Cl-rich apatites of 53% (J-1 rock sample only) and for typical F-apatites of 55% (the rest of the samples studied; see details below). Fragments of Durango F-apatite from the Cerro de Mercado mine were analyzed during the same sessions of track counting and LA-ICP-MS measurements. This famous mineral, with known age and more or less well-controlled chemical composition, was used to control the quality of AFT results obtained and as a primary standard for chlorine measurements in unknown apatites (taking a value of ~ 0.43 wt.% for Cl content; Goldoff *et al.*, 2012; Chew *et al.*, 2014). Single-grain AFT ages were calculated using the equations proposed by Hasebe *et al.* (2004, 2009), whereas 1σ -errors were obtained according to Abdullin *et al.* (2014, 2016a). Detailed information on our AFT and LA-ICP-MS experiments (including number of tracks counted, D -par values, ^{238}U and Cl concentrations, AFT ages, and analytical errors) is given in the Supplementary Appendix A1. After the LA-ICP-MS sessions, apatite crystals already analyzed were re-polished and re-etched to observe their fresh internal sections with the purpose to increase the number of confined tracks tested, following the same sample preparation procedure described above.

The LA-ICP-MS-based *in situ* fission-track method, fair to say that was introduced in 2000–2005 (Cox *et al.*, 2000; Svojtka and Košler, 2002; Hasebe *et al.*, 2004, 2009; Donelick *et al.*, 2005), is still in the development stage, or rather in a transition phase from the classical external detector method (EDM) to *in situ* technique (Vermeesch, 2017). After numerous experiments carried out in the past years, a LA-ICP-MS protocol for simultaneous U–Pb and AFT double dating plus multielemental analysis (rare earth elements, Y, Sr, Mn, Mg, Th, U, Cl) was established at the LEI Lab to be employed routinely in most unknown apatites (see details in Table 1).

RESULTS AND INTERPRETATIONS

For the Durango apatite used as a reference mineral, “absolute” mean ages of 30 ± 0.6 (1σ) Ma with dispersion of single-grain ages, $D = 0\%$ and chi-square probability test, $P(\chi^2) = 100\%$ (number of apatite grains dated, $\text{Ngr} = 12$) and of 29.4 ± 0.7 (1σ) Ma with $D = 0\%$ and $P(\chi^2) = 98\%$ ($\text{Ngr} = 10$) were obtained during two separate LA-ICP-MS sessions (grain ages and other details can be consulted in Supplementary Appendix A1). Both these values are slightly younger than its broadly accepted true age of 31.4 ± 0.5 (1σ) Ma (e.g., Green, 1985; McDowell *et al.*, 2005; Solé and Pi, 2005; Chew and Donelick, 2012; Jonckheere *et al.*, 2015). Hence, AFT ages obtained directly from unknown apatites were corrected to be given as “relative” ages based on the value of 31.4 Ma for the Durango apatite standard (following the methodology described in Hasebe *et al.*, 2004, 2009). This mathematical trick is recommended to obtain more reliable AFT ages and is basically equivalent to the ζ calibration (Hasebe *et al.*, 2004, 2013; Donelick *et al.*, 2005; Vermeesch, 2017) used in the conventional EDM (e.g., Hurford and Green, 1983; Wagner and Van den haute, 1992). The central (weighted-mean) AFT ages of the analyzed samples were calculated using the application RadialPlotter 8.3 written by Vermeesch (2009) and displayed as radial plots (Figures 3 and 4) (in statistics, known as Galbraith’s plots; Galbraith, 1988, 1994). To check the precision of chlorine measurements by LA-ICP-MS, the “1st Mine Discovery” apatite from Madagascar, a stunningly beautiful turquoise-colored mineral with a mean ^{206}Pb – ^{238}U age of 485–475 Ma (Thomson *et al.*, 2012; Chew *et al.*, 2014), was used. For this apatite, an average

Table 1. LA-ICP-MS protocol established at the LEI Lab (CGEO, UNAM) for simultaneous U–Pb and AFT double dating plus multielemental analysis (REE, Y, Sr, Mn, Mg, Th, U, and Cl).

ICP-MS operating conditions

| | |
|-------------------------|-----------------------------------------|
| Instrument | Thermo Scientific™ iCAP™ Qc |
| Forward power | 1,450 W |
| Carrier gas flow rate | ~ 1 L/min (Ar) and 0.35 L/min (He) |
| Auxiliary gas flow rate | ~ 1 L/min |
| Plasma gas flow rate | ~ 14 L/min |
| Nitrogen | ~ 3.5 mL/min |

Data acquisition parameters

| | |
|-----------------------|---------------------------------------------------------------------------------------------------------------------------------------------------------------------------------------------------------------------------------------------------------------------------------------------------------------------------------------------------------------------------------------------------------------------------------------------------------------------------------------------------------------------------------------------------------|
| Mode of operating | STD (standard mode) |
| Sampling scheme | –2NIST612–2MAD–1DUR–10apts– |
| Background scanning | 15 s |
| Data acquisition time | 35 s |
| Wash-out time | 15 s |
| Measured isotopes | ^{43}Ca ^{44}Ca ^{31}P ^{35}Cl ^{26}Mg ^{55}Mn ^{88}Sr ^{89}Y ^{139}La ^{140}Ce ^{141}Pr ^{146}Nd ^{147}Sm ^{153}Eu ^{157}Gd ^{159}Tb ^{163}Dy ^{165}Ho ^{166}Er ^{169}Tm ^{172}Yb ^{175}Lu ^{232}Th ^{238}U ^{204}Pb ^{206}Pb ^{207}Pb ^{208}Pb ^{202}Hg (total = 29) |

Laser ablation system

| | |
|------------------|-----------------------------------|
| Ablation cell | RESolution™ Laurin Technic S-155 |
| Model of laser | Resonetics RESolution™ LPX Pro |
| Wavelength | 193 nm (Excimer ArF) |
| Repetition rate | 4 Hz |
| *Energy density | *4 J/cm ² |
| Mode of sampling | spot diameter of 60 μm |

Note: REE: rare earth elements (La to Lu); MAD: “1st mine Discovery” U–Pb apatite standard from Madagascar; DUR: Durango F-apatite from the Cerro de Mercado mine (Mexico); apts: unknown apatites. (*): Constant laser pulse energy of 4 J/cm², which was measured on target with a Coherent™ apparatus. For larger apatites (e.g., 400 μm , such as those from some metamorphic rocks or from certain mineral deposits), accuracy and precision in Cl measurements, AFT dating, and U–Pb system can be significantly improved by employing larger spot sizes (e.g., 110 μm or above) as well as longer signal acquisition times (e.g., 55 s).

Cl content of 0.20 ± 0.01 (SD) wt.% was obtained in the LEI Lab, which is in line with the value of 0.22 ± 0.01 (SD) wt.% reported by Chew *et al.* (2014) also employing the LA-ICP-MS technique. Almost all the samples (except J-1) contain common F-apatites according to low levels of Cl (less than 0.2 wt.%; Figure 3) and small etch pits (D -par less than 2 μm ; Figures 4). It appears that etch pit size in apatite is not always linked to its halogen content (e.g., Barbarand *et al.*, 2003; our observations in the LEI Lab). In any case, D -par is widely accepted as a very practical semi-quantitative tool for the identification of different apatite specimens (Carlson *et al.*, 1999; Ketcham *et al.*, 1999; Donelick *et al.*, 2005; Lisker *et al.*, 2009). Annealing rates of fission tracks in apatite are apparently controlled by until-cell parameters, which can be “estimated” from the directly measured Cl content, though the content of certain trace elements (e.g., rare earth elements, Sr, Y) should also be taken into account (Barbarand *et al.*, 2003). Additional

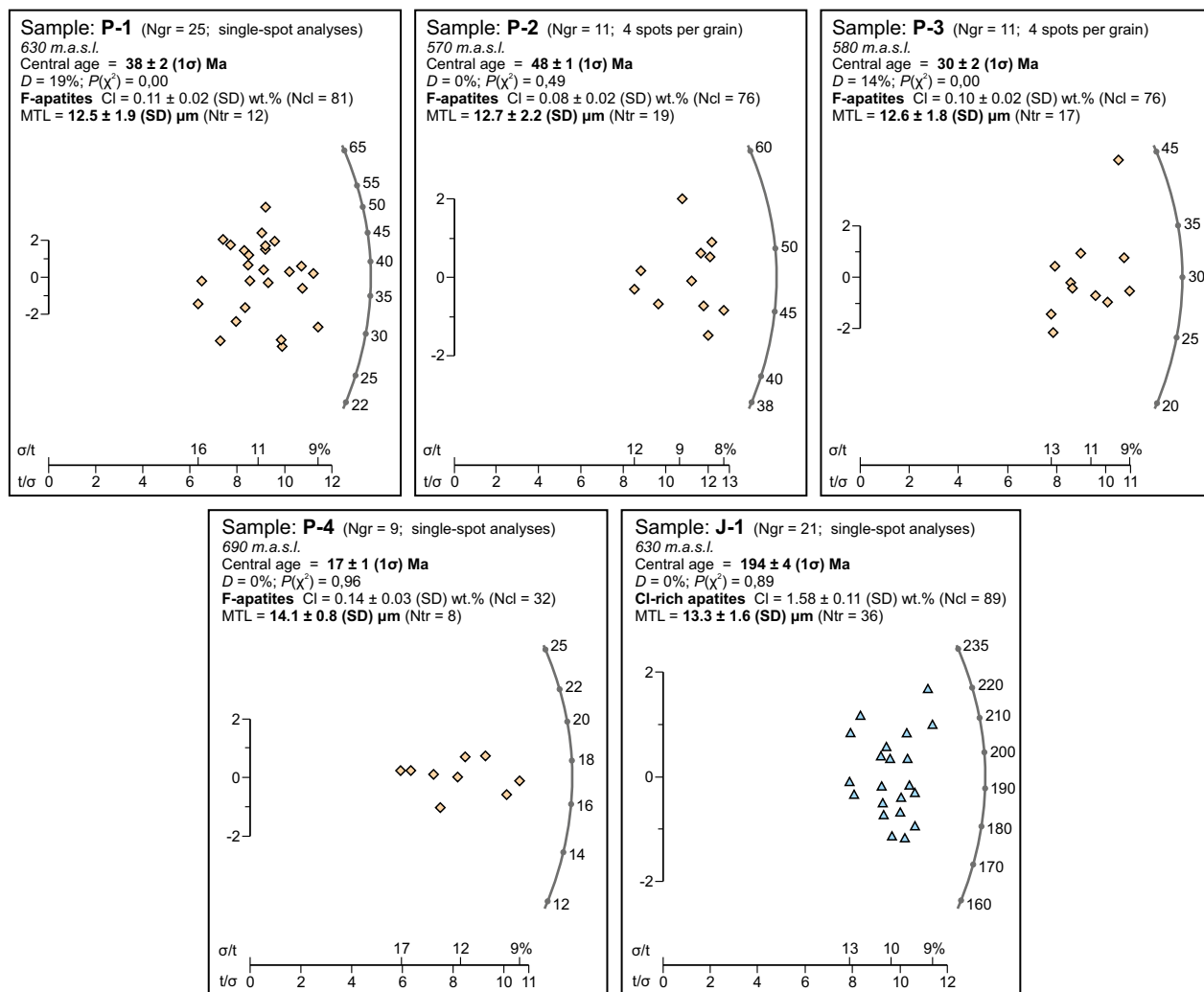


Figure 3. Radial plots displaying the AFT results for the CMC samples. P-1, P-2, P-3, and P-4 are late Permian granitoids/metagranitoids, and J-1 is a Jurassic subvolcanic sample. Ngr – number of apatite grains dated; Ncl – number of grains used for chlorine measurements by LA-ICP-MS; Ntr – number of confined tracks measured; D – dispersion of single-grain ages (%); $P(\chi^2)$ – chi-square probability test; MTL – mean track length. Note: only TINT-type confined tracks (*i.e.*, track-in-track; see details in Donelick *et al.*, 2005) were tested for MTL measurements.

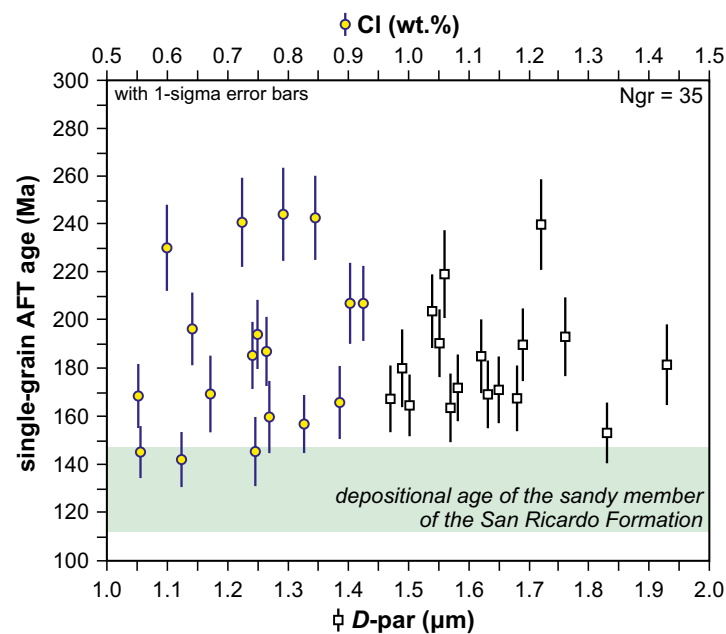
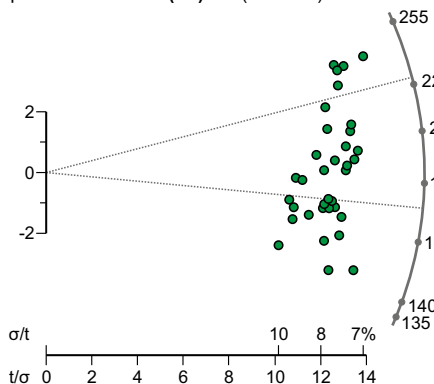
annealing experiments are highly recommended to better understand the mechanism and kinetics of fission-track annealing in apatites, especially in Cl-rich to Cl end-member varieties.

As shown in Figure 3, three late Permian igneous/meta-igneous samples (P-1, P-2 and P-3), despite their identical apatite compositions and roughly similar elevations, yielded dispersed AFT ages that are within a time span of *ca.* 50–25 Ma, and two of them apparently failed the chi-squared test. In spite of the large number of apatite sections observed (*ca.* 500 etched surfaces in each CMC rock sample), a few confined tracks were found to be measured (Ntr < 20 in most CMC samples and Ntr = 36 in J-1; Figure 3). This can be explained by either low U contents (Supplementary Appendix A1) or relatively young cooling ages, both factors that are crucial for generating low number of fission tracks. Mean confined track lengths (MTL) in these apatite groups range from 12.5 ± 1.9 (SD) to 12.7 ± 2.2 (SD) μm (Figure 3), which is common for samples from thermally undisturbed basement rocks (MTL of $12\text{--}13 \mu\text{m}$ with SD of $\sim 2 \mu\text{m}$; *e.g.*, Gleadow *et al.*, 1986). This implies that the samples P-1, P-2, and P-3 passed very slowly through the partial annealing zone (PAZ) of the AFT system (110 to

60 °C for F-apatites; Gleadow *et al.*, 1986; Green *et al.*, 1989; Donelick *et al.*, 2005). In this case, their mean AFT ages are actually “apparent cooling ages” and can hardly have any real geological meaning and, consequently, cannot be interpreted as indicating rapid cooling events *sensu stricto*. In contrast, apatites from samples P-4 and J-1 yielded longer MTL of 14.1 ± 0.8 (SD) and 13.3 ± 1.6 (SD) μm , respectively, and both rock samples undoubtedly passed the chi-square test (Figure 3). Therefore, these two samples, unlike the remaining three, may have cooled quite rapidly through their PAZ and, thus, can really reflect tectonic and magmatic events that occurred in the CMC region. The central AFT age of 17 ± 1 (1σ) Ma obtained from the late Permian sample P-4 can be interpreted as a cooling signal belonging to the middle-late Miocene event. The sample J-1 shows a mean AFT age of 194 ± 4 (1σ) Ma, which is significantly different from that obtained for other samples from the CMC. This age should be taken as the crystallization age for J-1 due to its apparent andesitic composition and high $P(\chi^2)$ (Figure 3). Besides, the AFT age obtained for J-1 is identical within error to the zircon U-Pb age of 196 ± 2 (2σ) Ma reported for the same sample by Ortega-Obregón *et al.* (2016). The number of

Sample: SR-1 (Ngr = 35; 1-3 spots per grain)

650 m a.s.l.

Central Age = 184 ± 5 (1 σ) Ma
D = 14%; $P(\chi^2) = 0,00$ D-par = 1.63 ± 0.12 (SD) μm
chlorine = 0.74 ± 0.11 (SD) wt.%
(F-apatites)peak 1 = 223 ± 10 (1 σ) Ma (27±10%)
peak 2 = 171 ± 5 (1 σ) Ma (73±10%)

Sample: SR-2 (Ngr = 39; 1-3 spots per grain)

870 m a.s.l.

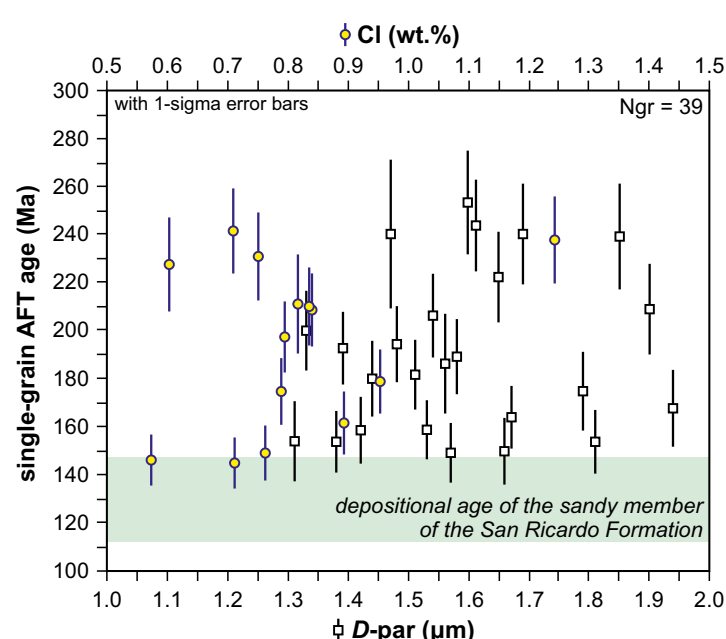
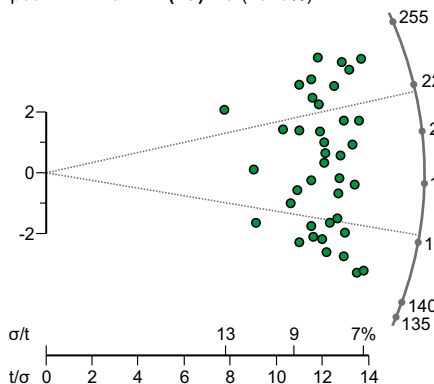
Central Age = 189 ± 5 (1 σ) Ma
D = 16%; $P(\chi^2) = 0,00$ D-par = 1.59 ± 0.17 (SD) μm
chlorine = 0.81 ± 0.16 (SD) wt.%
(F-apatites)peak 1 = 218 ± 5 (1 σ) Ma (51±9%)
peak 2 = 162 ± 4 (1 σ) Ma (49±9%)

Figure 4. Radial plots with AFT ages from the Berriasian to Aptian member of the San Ricardo Formation (SR-1 and SR-2, sampled in the uppermost level of the sandy member). Ngr – number of detrital apatite grains dated; D – age dispersion (%); $P(\chi^2)$ – chi-squared probability test. Binary plots displaying single-grain AFT ages vs. D-par values (or Cl contents) are also presented.

horizontally confined tracks measured in J-1 was high enough to be used in the interpretation of its complex thermal history (see the next section for details).

Most detrital apatite grains from the uppermost part of the Berriasian–Aptian sandy member of the San Ricardo Formation (SR-1 and SR-2) yielded single-grain AFT ages that are greater than its stratigraphic age, and no obvious positive correlation between D-par (or chlorine) and single-grain age was observed (Figure 4). The high amount of fission tracks preserved in apatite from these clastic samples (see U and ρ_s in Supplementary Appendix A1) allowed to test many track lengths (58 and 60 measurements in SR-1 and SR-2, respectively;

Figure 5). Apatites from SR-1 and SR-2 display short MTL of 12.4 ± 1.1 (SD) and 12 ± 1.1 (SD) μm , respectively. Track lengths with narrow distributions (SD of $\sim 1 \mu\text{m}$) and the absence of any bimodality in the histograms (Figure 5) can indicate that fission tracks in these detrital apatites were slightly annealed after deposition (e.g., Armstrong, 2005; Vermeesch *et al.*, 2006). Therefore, these sandstone samples reached the shallowest levels of the PAZ during burial diagenesis (probably, at most, only $\sim 70^\circ\text{C}$), which is in agreement with the stratigraphy of the study area where SR-1 and SR-2 are located in higher levels as compared to the dated Todos Santos Formation rocks (Figure 2), for which a maximum burial temperature of $80\text{--}90^\circ\text{C}$ has been proposed on the

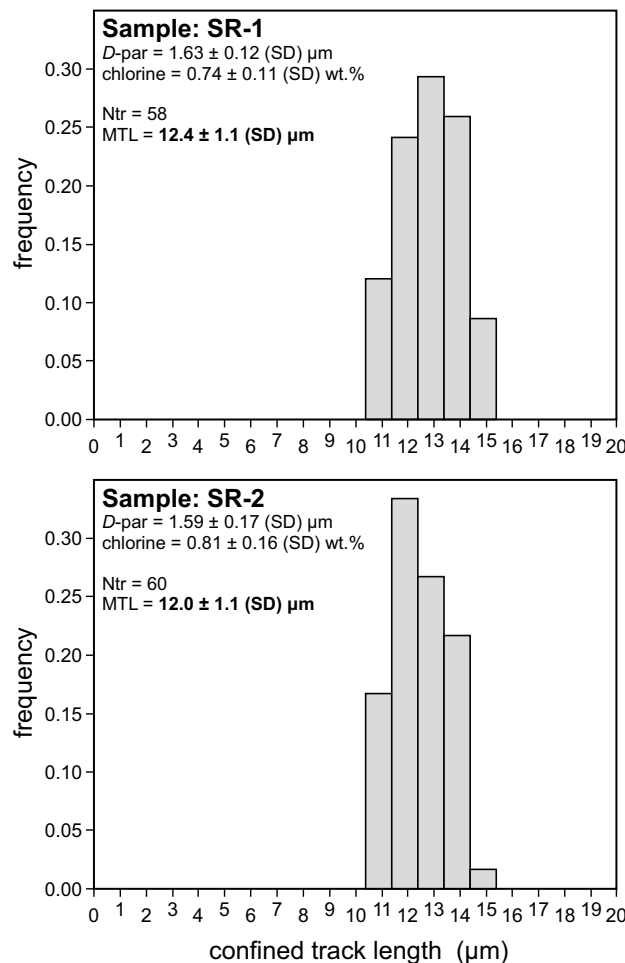


Figure 5. Observed (measured) fission-track length distributions for SR-1 and SR-2, shown as histograms. Ntr – number of track lengths measured; MTL – mean track length. Note: only TINT-type confined tracks (track-in-track; see Donelick *et al.*, 2005) were tested for MTL measurements.

basis of thermal history modeling (Abdullin *et al.*, 2016a; for more details, see also the next section). These results suggest that detrital apatites from SR-1 and SR-2 were not fully reset for AFT chronometry by burial-related re-heating during diagenesis (Figure 4); hence, their unreset AFT ages (*i.e.*, ages with provenance signals) may be crucial to define indirectly certain cooling episodes occurred in the CMC during the Triassic to Jurassic period.

Identical central AFT ages of 184 ± 5 (1σ) and of 189 ± 5 (1σ) Ma were obtained for SR-1 (Ngr = 35) and SR-2 (Ngr = 39), respectively (Figure 4), which likely have no real geological significance due to their scattered single-grain ages of 253 ± 21 (1σ) to 142 ± 12 (1σ) Ma (see Supplementary Appendix A1) and $P(\chi^2)$ of 0%. Therefore, it is necessary to decompose these AFT results into groups of component distributions, which may provide useful information about the cooling events that took place in the source areas (*e.g.*, Armstrong, 2005; Donelick *et al.*, 2005; Vermeesch *et al.*, 2006; Lisker *et al.*, 2009). The data were decomposed using RadialPlotter 8.3 (Vermeesch, 2009) based on the statistics of Galbraith and Green (1990). As a result, two equally important AFT age peaks of 223 ± 10 (1σ) to 218 ± 5 (1σ) and of 171 ± 5 (1σ) to 162 ± 4 (1σ) Ma were obtained (Figure 4), which could be interpreted as Triassic and Jurassic cooling signals derived from the CMC source area.

DISCUSSION

Late Triassic cooling event

The oldest AFT age peaks of 223 ± 10 (1σ) and 218 ± 5 (1σ) Ma obtained from the San Ricardo Formation indicate that a Triassic cooling event took place in the CMC, the source area from which the sediments were entirely derived (*e.g.*, Quezada-Muñetón, 1983; Sánchez *et al.*, 2004; Abdullin *et al.*, 2016b). Triassic cooling signals were also obtained directly from the CMC on the basis of numerous medium-temperature thermochronometric studies. For example, Torres *et al.* (1999) compiled K-Ar biotite ages from 261 ± 10 (2σ) to 239 ± 5 (2σ) Ma, the youngest of which may be interpreted as Triassic cooling ages. Schaaf *et al.* (2002) also demonstrated, using Rb-Sr ages of 244 ± 12 (2σ) to 214 ± 11 (2σ) Ma obtained for biotite-whole-rock pairs, that an important cooling event occurred in the CMC during the Triassic. These systems in micas have closure temperatures of 350 – 300 °C (*e.g.*, Faure and Mensing, 2005). Triassic cooling ages were also verified by apatite U-Pb thermochronology tested on some CMC samples that yielded U-Pb ages of \sim 250–230 Ma (Ortega-Obregón *et al.*, 2016), which display cooling times through \sim 550–400 °C paleoisotherms (*e.g.*, Cochrane *et al.*, 2014). However, Triassic AFT ages obtained in this study indicate cooling episodes through significantly colder paleoisotherms (taking \sim 120–100 °C as an effective closure temperature in F-apatites). All these nearly similar cooling ages imply that the CMC was partially uplifted and eroded already during the Late Triassic (at *ca.* 230–210 Ma). Some detrital apatite grains from the Todos Santos Formation (Figure 2) also yielded Triassic AFT ages (Abdullin *et al.*, 2016a). Hence, the depositional age for the Todos Santos Formation, overlying the CMC, could be extended up to the Triassic (\sim 230 Ma as the age of the lowermost strata in some parts of SE Mexico), as it was previously suggested by several authors (*e.g.*, Salvador, 1987; Padilla y Sánchez, 2007; Pérez-Gutiérrez *et al.*, 2009). The \sim 230–210 Ma cooling period is coeval with the initial breakup of Pangea during the Late Triassic, which in turn confirms that the CMC, as well as the whole Maya block, were involved in this global-scale geodynamic activity (Michalzik, 1991; Dickinson and Lawton, 2001; Steiner, 2005; Bird and Burke, 2006; Padilla y Sánchez, 2007; Martini and Ortega-Gutiérrez, 2016).

Early Jurassic magmatism

Although Jurassic igneous rocks have not been separately plotted on available geological maps, there is evidence for the existence of Jurassic magmatic activity in the CMC. For example, a Middle–Late Jurassic magmatism (175–140 Ma) was suggested for the CMC area by Damon *et al.* (1981) on the basis of reset K-Ar biotite ages from late Permian granitoids as well as on the dating of andesite dykes and hydrothermally altered rocks. More recent geochronological data (*e.g.*, Schaaf *et al.*, 2002; Godínez-Urban *et al.*, 2011; Ortega-Obregón *et al.*, 2016; this study), however, indicate that this magmatic event took place in the Early Jurassic (200–180 Ma). Sample J-1 is of volcanic, or rather of subvolcanic, origin. Its AFT age of 194 ± 4 (1σ) Ma (Figure 3), together with an $^{40}\text{Ar}/^{39}\text{Ar}$ date of 186 ± 2 (2σ) Ma on hornblende and a zircon U-Pb age of 191 ± 3 (2σ) Ma reported recently for the southern CMC area (see details in Godínez-Urban *et al.*, 2011), as well as a zircon U-Pb age of 196 ± 2 (2σ) Ma for J-1 (Ortega-Obregón *et al.*, 2016) suggest that the main period of the Jurassic magmatic event in the CMC could be reduced to *ca.* 200–190 Ma. The Early Jurassic magmatism detected within the territory of Chiapas confirms that the Maya block stores signals of the Early–Middle Jurassic Nazas volcanic arc (*ca.* 200–160 Ma; *e.g.*, Godínez-Urban *et al.*, 2011; Rubio-Cisneros and Lawton, 2011).

Middle Jurassic tectonic event

Both AFT age peaks at 171 ± 5 (1 σ) and 162 ± 4 (1 σ) Ma obtained for SR-1 and SR-2 samples from the San Ricardo Formation (Figure 4) suggest that a Middle Jurassic cooling event affected the CMC, at least partly. It is necessary to take into account that these cooling peaks may be slightly overestimated due to the presence of some detrital apatites with Early Jurassic AFT ages (Figure 4), which could have been derived from Early Jurassic volcanic sources as well (e.g., Abdullin *et al.*, 2016b). These age peaks, nevertheless, are in line with the age of the strike-slip event along the Sierra de Juárez mylonitic belt (southern Mexico), which was determined as 169 ± 2 (2 σ) Ma based on muscovite $^{40}\text{Ar}/^{39}\text{Ar}$ ages (Alaniz-Alvarez *et al.*, 1996). Recently, Martini *et al.* (2016) also identified a Middle Jurassic exhumation signal of 172–162 Ma from the Matanza fault to the north of the late Paleozoic Totoltepec pluton (southern Mexico). Within the Chiapas region, an important AFT age peak of 163 ± 3 (1 σ) Ma was obtained from non- to slightly annealed apatites from four Todos Santos Formation sandstones (Figure 2) studied by Abdullin *et al.* (2016a). This AFT age peak as well as the AFT peaks of 171 ± 5 (1 σ) and 162 ± 4 (1 σ) Ma obtained for the San Ricardo Formation (this study) belong to the same Middle Jurassic tectonic event that can be identified elsewhere in southern Mexico (e.g., Alaniz-Alvarez *et al.*, 1996; Martini *et al.*, 2016). The Middle Jurassic cooling period with an approximate age of 170–160 Ma was triggered by continental rifting at the beginning of the opening of the Gulf of Mexico (Alaniz-Alvarez *et al.*, 1996; Bird *et al.*, 2005; Bird and Burke, 2006; Godínez-Urban *et al.*, 2011). In other words, Jurassic cooling ages derive from extensional processes that affected the southern margins of the Gulf of Mexico. This is registered as highly variable thicknesses of Triassic(?) to Jurassic red beds, which can be linked to graben-type geometries essentially related to extensional processes associated with continental rifting during the opening of the Gulf of Mexico (Meneses-Rocha, 1985, 1991, 2001; Blair, 1987; Sánchez-Montes de Oca, 2006; Padilla y Sánchez, 2007; Witt *et al.*, 2012; Martini and Ortega-Gutiérrez, 2016).

Late Cretaceous–Paleocene orogeny

During the Late Jurassic period, a marine transgression took place in the territories now occupied by Chiapas and the Yucatán platform, between which the Late Jurassic to Late Cretaceous basins of south-eastern Mexico began to form (e.g., Meneses-Rocha, 1985, 1991, 2001; Sánchez-Montes de Oca, 2006; Padilla y Sánchez, 2007). The well-exposed base of the Oxfordian–Aptian San Ricardo Formation is an important register of this regional transgression (Quezada-Muñetón, 1983; Blair, 1987; Sánchez *et al.*, 2004). The early stage of the development of these basins continued until the Albian–Santonian period, during which an extensive carbonate platform was established (the Sierra Madre Formation), well preserved in the Sierra Madre Oriental as well as in the Sierra de Chiapas (Rosales-Domínguez *et al.*, 1997; Rosales-Domínguez, 1998; Meneses-Rocha, 2001; Sánchez-Montes de Oca, 2006; Fitz-Díaz *et al.*, 2017). Previous thermal history modeling of the study area (Figure 6a; Abdullin *et al.*, 2016a) indicates that burial-related heating of the Todos Santos Formation during its long-term diagenesis, and particularly during the development of the Cretaceous platform, was sufficient to reset the AFT system in the majority of detrital apatites. A Late Cretaceous–early Paleogene orogeny, previously proposed for the area of Chiapas on the basis of stratigraphic and structural studies (e.g., Gutiérrez-Gil, 1956; Sánchez-Montes de Oca, 1979, 2006; Carfantán, 1981, 1985; Moravec, 1983; Meneses-Rocha, 1985, 1991, 2001; Burkart *et al.*, 1987), has been confirmed by AFT thermochronology applied for the Todos Santos Formation sandstones (Figure 6a; Abdullin *et al.*, 2016a). All the aforementioned authors related this orogenic event to the Laramide orogeny. Nonetheless, in

order to avoid any confusion, it may be more correct to name the event occurred in Chiapas as the Laramide *sensu lato*, a term proposed by Garduño-Martínez *et al.* (2015). Both best-fit curves on AFT analysis-derived thermal models with high values of goodness-of-fit between the measured and model ages (GOF) and goodness-of-fit between the measured and model confined track lengths (GOF K-S) (Figure 6a) suggest that this thermo-tectonic activity affected the CMC area during the Late Cretaceous to Paleocene (~85–80 to 60–55 Ma). However, as it was already proposed in previous works (Meneses-Rocha, 1985, 1991, 2001; Padilla y Sánchez, 2007), the deformation style of this tectonic event in Chiapas may be different if compared to its roughly contemporaneous analogue from central and northern Mexico (e.g., Garduño-Martínez *et al.*, 2015; Fitz-Díaz *et al.*, 2017). Finally, there is abundant evidence that the CMC area was repeatedly uplifted and eroded during the Laramide *sensu lato* (i.e., during the Late Cretaceous–Paleocene) and, as result, conglomerates and sandstones at the base of the sedimentary cover in the Gulf of Tehuantepec (Figure 1) were deposited in the Late Cretaceous (e.g., Sánchez-Barreda, 1981; Pedrazzini *et al.*, 1982; Meneses-Rocha, 2001; Sánchez-Montes de Oca, 2006; Morán-Zenteno *et al.*, 2009). In other words, Late Cretaceous–Holocene clastic sediments of the Gulf of Tehuantepec were partially derived from the CMC.

Due to a relatively close localization of sample J-1 to the Todos Santos Formation sandstones already analyzed by AFT thermochronology (Figure 2), its thermal history can be constructed as a predictive model on the basis of modeling results previously reported for the Todos Santos Formation (Figures 6a and 6b; Abdullin *et al.*, 2016a); though, it should be noted that sample J-1 was collected from a stratigraphically lower level than those from the Todos Santos Formation. It is well known that fission tracks in Cl-apatite specimens are significantly more resistant to thermal annealing as compared with tracks from typical F-apatites (Carlson *et al.*, 1999; Ketcham *et al.*, 1999; Barbarand *et al.*, 2003; Donelick *et al.*, 2005). For example, for apatites displaying $D_{\text{par}} \geq 3 \mu\text{m}$ or with $\text{Cl} \geq 3 \text{ wt.}\%$, Donelick *et al.* (2005) postulated that fission tracks begin to anneal at $\sim 90^\circ\text{C}$ and experience total annealing at temperatures greater than 160°C . The Early Jurassic sample J-1 is characterized by Cl-rich apatites with Cl contents of 1.58 ± 0.11 (SD) wt.% (Figures 3 and 6b). This means that, first of all, these apatites have elevated closure temperatures (either PAZ or effective closure temperatures) and, secondly, the PAZ in J-1-derived apatites should be slightly wider and “hotter” as compared to the PAZ of 110 – 60°C in common F-apatites (Gleadow *et al.*, 1986; Green *et al.*, 1989; Donelick *et al.*, 2005). According to this premise, for J-1 we can hypothetically assume a PAZ of ~ 130 – 70°C . For this reason, burial-related heating was not sufficient to reset the AFT ages in J-1 (J-1 reached only the uppermost part of the PAZ, as shown in Figure 6b) but the temperature was high enough to partially anneal some fission tracks, finally yielding a bimodal length distribution with MTL of 13.3 ± 1.6 (SD) μm (Figures 3 and 6b), which is quite common for rock samples that experienced complex thermal histories (Gleadow *et al.*, 1986; Wagner and Van den haute, 1992; Donelick *et al.*, 2005; Vermeesch *et al.*, 2006; Lisker *et al.*, 2009). The bimodality in the track length distribution in apatite from J-1 was formed during the development of the Cretaceous platform in southeastern Mexico.

Cenozoic tectonic evolution

The Oligocene rapid cooling event, which could have been triggered by the arrival of the Chortís block in front of the Gulf of Tehuantepec and, consequently, by its collision with the Maya block (Ratschbacher *et al.*, 2009; Witt *et al.*, 2012), was not identified in the northern CMC region. The AFT data from CMC samples P-1, P-2, and P-3 (Figures 2 and 3), as well as two thermal histories simulated for the

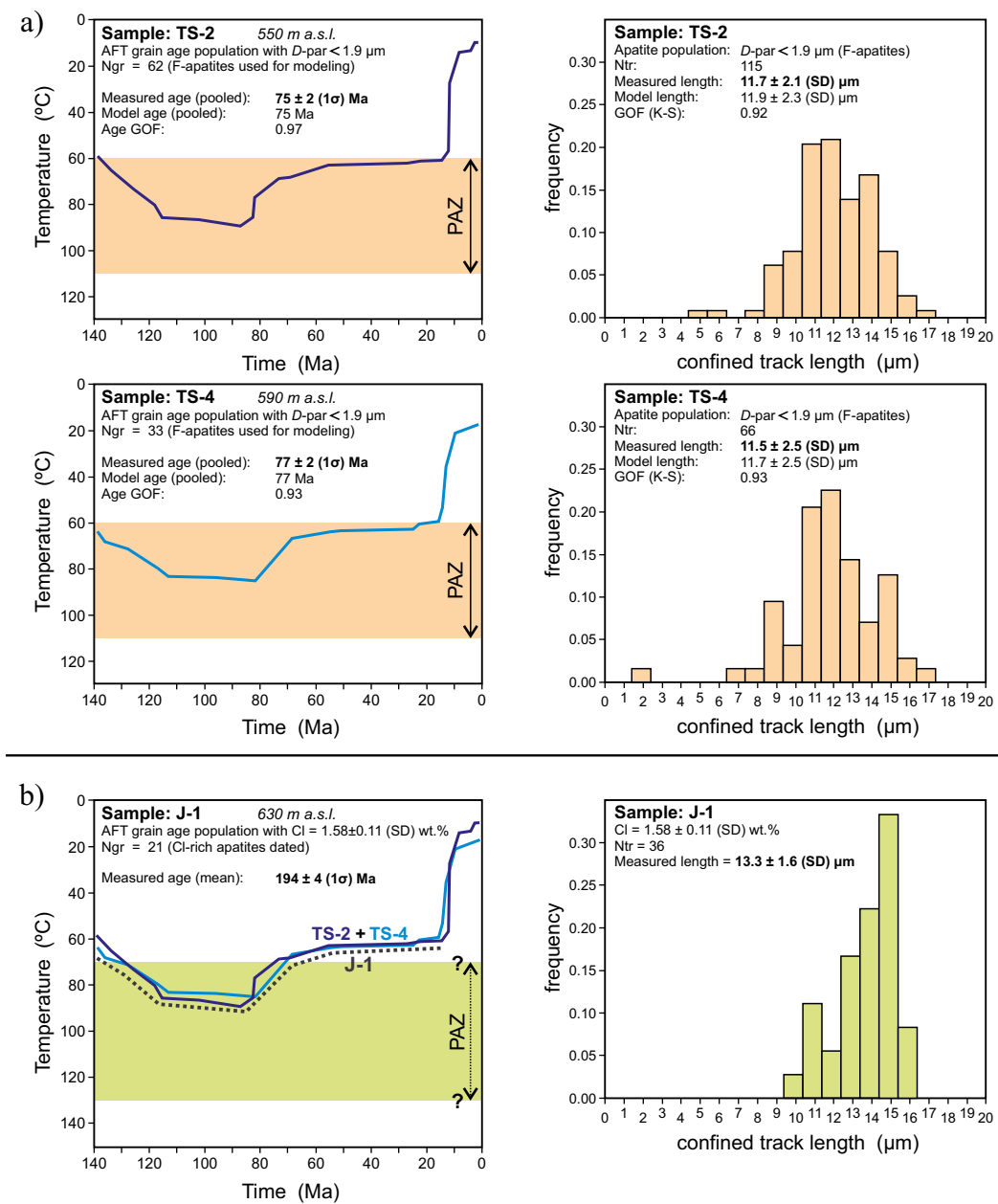


Figure 6. (a) Thermal modeling results for samples T-2 and T-4 (see location in Figure 2) from the Todos Santos Formation (taken from Abdullin *et al.*, 2016a). Note that only best-fit curves are presented. The simulation of time-temperature histories was performed using the HeFTy 1.8.0 software of Ketcham (2005) based on the annealing model proposed by Ketcham *et al.* (2007). Modeling was carried out for a defined population of detrital apatites dated and confined tracks tested with D_{par} values of less than 1.9 μm , which mainly correspond to F-apatites (etching protocol: 5.5 M HNO_3 at 21 $^{\circ}\text{C}$ for 20 s). Ngr – number of dated grains with $D_{\text{par}} < 1.9 \mu\text{m}$; Ntr – number of tracks measured in apatites with $D_{\text{par}} < 1.9 \mu\text{m}$; Age GOF – goodness-of-fit between the measured and model ages; GOF (K-S) – goodness-of-fit between the measured and model confined track lengths; (K-S) is the Kolmogorov-Smirnov test; PAZ – partial annealing zone for F-apatites (110 to 60 $^{\circ}\text{C}$; Gleadow *et al.*, 1986; Green *et al.*, 1989; Donelick *et al.*, 2005). (b) Predictive modeling of the thermal history of Cl-rich apatites from sample J-1 based on the results from TS-2 and TS-4. PAZ was hypothetically assumed as *ca.* 130–70 $^{\circ}\text{C}$ (see text for more details). The number of tested tracks in J-1 was too low to construct a HeFTy-based time-temperature history, because around 100 to 150 track length measurements are recommended for samples that display complex thermal histories (*e.g.*, exhumation–burial–exhumation, like J-1). Note: only TINT-type confined tracks (*i.e.*, track-in-track) were tested for MTL measurements.

Todos Santos Formation (Abdullin *et al.*, 2016a; see best-fit curves in Figure 6a), suggest that the Eocene–early Miocene was likely a period of tectonic calm in the north-central CMC area. Recent provenance studies performed in some Cenozoic units from the internal Sierra de Chiapas (Witt *et al.*, 2012; Abdullin *et al.*, 2016b) support this hypothesis, because Eocene clastic sediments were definitely not derived from the CMC source area. Meneses-Rocha (1985, 2001) proposed

that Eocene–Oligocene sediments in Chiapas were mainly derived from Central Guatemala, a hypothesis that was in part confirmed by provenance analyses performed on the Ypresian–Lutetian(?) El Bosque Formation (Abdullin *et al.*, 2016b). In a similar way, we can speculate that Oligocene clastic materials of Chiapas were predominantly derived from southern source areas, which is also supported by an apparent south-to-north marine regression during this time (Meneses-Rocha,

1985, 2001; Quezada-Muñetón, 1987). The Oligocene column of the Sierra de Chiapas is characterized by siliciclastic deep-basin sediments as well as by carbonate and mixed platforms developed in shallow water environments (Quezada-Muñetón, 1987; Meneses-Rocha, 2001; Witt *et al.*, 2012). Most Oligocene sediments of the northern Sierra de Chiapas, therefore, were probably derived from regions located farther south; the Guatemala Suture Zone (Figure 1), also known as the Guatemala Suture Complex (Martens *et al.*, 2012), is a good candidate for the main source region (Meneses-Rocha, 1985, 1991, 2001). Finally, it may be proposed that the CMC has not experienced any significant tectonic uplift during the Eocene to early Miocene period. Oligocene-aged abrupt cooling signals from the southernmost section of the CMC require a strong confirmation in further thermochronological studies.

Rapid cooling signals, corresponding to the middle to late Miocene Chiapanecan orogeny (Sánchez-Montes de Oca, 1979, 2006; Meneses-Rocha, 1985, 2001; Padilla y Sánchez, 2007; Guzmán-Speziale, 2010), were best detected in the thermochronological studies of Witt *et al.* (2012), based on AFT analyses and apatite (U-Th-Sm)/He dating. Both thermal histories modeled from the Todos Santos Formation also reveal this recent tectonic activity, showing very rapid cooling of apatites from the upper PAZ (65–60 °C) to the surface temperature (Figure 6a; Abdullin *et al.*, 2016a). In this study, such a young cooling age was extracted only for P-4 (17 ± 1 Ma; Figure 3), which was sampled closer to the Tonalá Shear Zone as compared to other analyzed samples (Figure 2). Its cooling signal is roughly coeval with the activation time of the Tonalá Shear Zone, along which many plutons were also emplaced during the middle to late Miocene (e.g., Molina-Garza *et al.*, 2015). Thereby, fast exhumation of the CMC, or rather of the entire territory of Chiapas, started at the middle-late Miocene. This thermo-tectonic event, together with the Pliocene to present magmatism in the Sierra de Chiapas, was important for the development of geological structures as well as of the steep present-day topography (~20 to ~4,100 m a.s.l.) in Chiapas (e.g., Meneses-Rocha, 2001; Witt *et al.*, 2012). Both events, and especially the Chiapanecan orogeny, caused extensive erosion and abundant terrigenous sediment supply from the Chiapas territory to the north into the Tabasco plain (Sánchez-Montes de Oca, 1979, 2006; Quezada-Muñetón, 1987; Meneses-Rocha, 2001; Padilla y Sánchez, 2007). In terms of regional tectonics, the middle-late Miocene Chiapanecan event is most likely controlled by the interaction of the North American, Caribbean, and Cocos plates (Meneses-Rocha, 2001; Padilla y Sánchez, 2007; Guzmán-Speziale, 2010; Authemayou *et al.*, 2011; Witt *et al.*, 2012).

CONCLUSIONS AND RECOMMENDATIONS

The new fission-track ages reported in this study, together with some previous data on the tectonic history of southeastern Mexico, strongly indicate that the CMC, as well as the whole Maya block, have experienced a complex long-term tectonic evolution. For southeastern Mexico, at least five post-Permian tectonic and magmatic events may be proposed: (1) a Late Triassic (230–210 Ma) cooling event, probably linked to the initial breakup of Pangea; (2) Early Jurassic (from 200 to 190–180 Ma) magmatism that is related to the Nazas volcanic arc; (3) a Middle Jurassic tectonic event with an age of 170–160 Ma that was likely triggered by continental rifting at the beginning of the opening of the Gulf of Mexico; (4) a Late Cretaceous–Paleocene orogenic event, which can actually represent the southernmost continuation of the Laramide *sensu lato* that affected central and northern Mexico; and (5) the middle to late Miocene Chiapanecan orogeny that seems to be tectonically controlled by the interaction of the North American, Caribbean, and Cocos plates.

The tectonic history of the CMC is somewhat "entangled" as result of the debatable results and ideas proposed for its Cenozoic evolution (Ratschbacher *et al.*, 2009; Witt *et al.*, 2012; Abdullin *et al.*, 2016a; this study). For example, Ratschbacher *et al.* (2009) suggested that the CMC region exhumed rapidly during the Oligocene, likely due to the hypothetical arrival of the Chortís block in front of the Gulf of Tehuantepec area. However, the results of recent studies (Witt *et al.*, 2012; Abdullin *et al.*, 2016a; this study) indicate that, at least, the central and northern portions of the CMC display no abrupt exhumation signals for this period of time. This controversy is due to the absence of systematic and detailed studies along the entire CMC. Additional thermochronological studies are also recommended. These integrated studies should be based on those methods that have closure temperatures below 300 °C such as apatite and zircon fission-track analyses and helium dating, because other techniques with higher closure temperatures will most likely yield either Triassic or Jurassic ages, which are typical for the CMC. Also, these studies should be performed across several sections of the CMC, *i.e.*, in the northern, central, and southern CMC, because the southernmost CMC may store Oligocene cooling ages *sensu stricto*. Furthermore, these studies can be accompanied by provenance analyses in specific clastic successions, in particular from Cenozoic units that crop out within the central and northern areas of the Sierra de Chiapas.

ACKNOWLEDGEMENTS

The authors are very grateful to Juan Tomás Vázquez Ramírez, Manuel Albarrán Murillo, Oscar Aguilar Moreno, and Ofelia Pérez Arvizu (all from CGEO, UNAM) for their help with sample preparation for apatite fission-track analyses. Professor Stuart Thomson (University of Arizona) is acknowledged for sharing some fragments of the Madagascar apatite. F.A. thanks DGAPA UNAM for a 2016–2018 postdoctoral fellowship. This study was financially supported by PAPIIT UNAM [grant IN103417] to Luigi Solari. Dr. Thierry Calmus (ERNO, UNAM) and Professor Cesar Witt (Lille-1 University, France) are acknowledged for their useful observations that improved our manuscript significantly. Dr. Peter Schaa (Editor-in-Chief of RMCG) helped us a lot with the correction of several grammatical errors.

SUPPLEMENTARY MATERIAL

Supplementary Appendix A1 with detailed information on apatite fission-track and LA-ICP-MS experiments performed at LEI Lab (CGEO, UNAM) can be found at the journal web site <<http://rmcg.unam.mx/>>, in the table of contents of this issue.

REFERENCES

Abdullin, F., Solé, J., Solari, L., 2014, Datación mediante trazas de fisión y análisis multielemental con LA-ICP-MS del fluorapatito de Cerro de Mercado (Durango, México): Revista Mexicana de Ciencias Geológicas, 31(3), 395–406.

Abdullin, F., Solé, J., Meneses-Rocha, J.D.J., Solari, L., Shchepetilnikova, V., Ortega-Obregón, C., 2016a, LA-ICP-MS-based apatite fission track dating of the Todos Santos Formation sandstones from the Sierra de Chiapas (SE Mexico) and its tectonic significance: International Geology Review, 58(1), 32–48.

Abdullin, F., Solé, J., Solari, L., Shchepetilnikova, V., Meneses-Rocha, J.J., Pavlinova, N., Rodríguez-Trejo, A., 2016b, Single-grain apatite geochemistry of Permian–Triassic granitoids and Mesozoic and Eocene sandstones from Chiapas, southeast Mexico: implications for sediment

provenance: *International Geology Review*, 58(9), 1132-1157.

Alaniz-Álvarez, S.A., van der Heyden, P., Nieto-Samaniego, A.F., Ortega-Gutiérrez, F., 1996, Radiometric and kinematic evidence for Middle Jurassic strike-slip faulting in southern Mexico related to the opening of the Gulf of Mexico: *Geology*, 24(5), 443-446.

Armstrong, P.A., 2005, Thermochronometers in Sedimentary Basins: Reviews in Mineralogy and Geochemistry, 58, 499-525, DOI:10.2138/rmg.2005.58.19.

Authemayou, C., Brocard, G., Teyssier, C., Simon-Labré, T., Gutiérrez, A., Chiquín, E.N., Morán, S., 2011, The Caribbean-North America-Cocos Triple Junction and the dynamics of the Polochic-Motagua fault systems: Pull-up and zipper models: *Tectonics*, 30(3), DOI:10.1029/2010TC002814

Barbarand, J., Carter, A., Wood, I., Hurford, T., 2003, Compositional and structural control of fission-track annealing in apatite: *Chemical Geology*, 198(1), 107-137.

Bird, D., Burke, K., 2006, Pangea breakup: Mexico, Gulf of Mexico, and Central Atlantic Ocean, in *SEG Technical Program Expanded Abstracts 2006: Society of Exploration Geophysicists*, 1013-1017a.

Bird, D.E., Burke, K., Hall, S.A., Casey, J.F., 2005, Gulf of Mexico tectonic history: Hotspot tracks, crustal boundaries, and early salt distribution: *American Association of Petroleum Geologists Bulletin*, 89(3), 311-328.

Blair, T.C., 1987, Tectonic and hydrologic controls on cyclic alluvial fan, fluvial, and lacustrine rift-basin sedimentation, Jurassic-Lowermost Cretaceous Todos Santos Formation, Chiapas, Mexico: *Journal of Sedimentary Research*, 57(5), 845-862.

Burkart, B., Deaton, B.C., Dengo, C., Moreno, G., 1987, Tectonic wedges and offset Laramide structures along the Polochic fault of Guatemala and Chiapas, Mexico: reaffirmation of large Neogene displacement: *Tectonics*, 6(4), 411-422.

Carfantan, J.C., 1981, Evolución estructural del sureste de México, Paleogeografía e historia tectónica de las zonas internas mesozoicas: *Revista Mexicana de Ciencias Geológicas*, 5(2), 207-216.

Carfantan, J.C., 1985, Du système cordillerain Nord-Américain au domaine Caraïbe. Étude géologique du Mexique méridional: Université de Savoie, France, Ph.D. Thesis, 558 pp.

Carlson, W.D., Donelick, R.A., Ketcham, R.A., 1999, Variability of apatite fission-track annealing kinetics: I. Experimental results: *American Mineralogist*, 84(9), 1213-1223.

Chew, D.M., Donelick, R.A., 2012, Combined apatite fission-track and U-Pb dating by LA-ICP-MS and its application in apatite provenance analysis, in Sylvester P. (ed.), *Quantitative Mineralogy and Microanalysis of Sediments and Sedimentary Rocks*: Mineralogical Association of Canada, Short Course 42, 219-247.

Chew, D.M., Donelick, R.A., Donelick, M.B., Kamber, B.S., Stock, M.J., 2014, Apatite Chlorine Concentration Measurements by LA-ICP-MS: Geostandards and Geoanalytical Research, 38(1), 23-35.

Cisneros de León, A., Weber, B., Ortega-Gutiérrez, F., González-Guzmán, R., Maldonado, R., Solari, L., Schaaf, P., Manjarrez-Juárez, R., 2017, Grenvillian massif-type anorthosite suite in Chiapas, Mexico: Magmatic to polymetamorphic evolution of anorthosites and their Ti-Fe ores: *Precambrian Research*, 295, 203-226.

Cochrane, R., Spikings, R.A., Chew, D., Wotzlaw, J.F., Chiaradia, M., Tyrrell, S., Schaltegger, U., Van der Lelij, R., 2014, High temperature (> 350 °C) thermochronology and mechanisms of Pb loss in apatite: *Geochimica et Cosmochimica Acta*, 127, 39-56.

Cox, R., Košler, J., Sylvester, P., Hodych, P., 2000, Apatite fission-track (FT) dating by LAM-ICP-MS analysis, in *Goldschmidt Conference*, Oxford, UK: *Journal of Conference Abstracts*, 5(2), p. 322.

Damon, P.E., Shafiqullah, M., Clark, K.F., 1981, Age trends of igneous activity in relation to metallogenesis in the southern Cordillera, in Dickinson, W.R., Payne, W.D. (eds.), *Relations of Tectonics to Ore Deposits in the Southern Cordillera*: Tucson, Arizona, Arizona Geological Society Digest, 14, 137-153.

Dengo, G., 1985, Mid America: Tectonic setting for the Pacific margin from southern México to northwestern Colombia, in *The ocean basins and margins*: Springer US, 123-180.

Dickinson, W.R., Lawton, T.F., 2001, Carboniferous to Cretaceous assembly and fragmentation of Mexico: *Geological Society of America Bulletin*, 113(9), 1142-1160.

Donelick, R.A., O'Sullivan, P.B., Ketcham, R.A., 2005, Apatite fission-track analysis: *Reviews in Mineralogy and Geochemistry*, 58(1), 49-94.

Ehlers, T.A., Farley, K.A., 2003, Apatite (U-Th)/He thermochronometry: methods and applications to problems in tectonic and surface processes: *Earth and Planetary Science Letters*, 206(1), 1-14.

Estrada-Carmona, J., Weber, B., Hecht, L., Martens, U., 2009, PT trajectory of metamorphic rocks from the central Chiapas Massif Complex: the Cuspea Unit, Chiapas, Mexico: *Revista Mexicana de Ciencias Geológicas*, 26(1), 243-259.

Estrada-Carmona, J., Weber, B., Martens, U., López-Martínez, M., 2012, Petrogenesis of Ordovician magmatic rocks in the southern Chiapas Massif Complex: relations with the early Palaeozoic magmatic belts of northwestern Gondwana: *International Geology Review*, 54(16), 1918-1943.

Faure, G., Mensing, T.M., 2005, *Isotopes: Principles and applications*: New York, John Wiley & Sons, 897 pp.

Fitz-Díaz, E., Lawton, T.F., Juárez-Arriaga, E., Chávez-Cabello, G., 2017, The Cretaceous-Paleogene Mexican orogen: Structure, basin development, magmatism and tectonics: *Earth-Science Reviews*, doi:10.1016/j.earscirev.2017.03.002.

Galbraith, R.F., 1988, Graphical display of estimates having differing standard errors: *Technometrics*, 30(3), 271-281.

Galbraith, R.F., 1994, Some applications of radial plots: *Journal of the American Statistical Association*, 89(428), 1232-1242.

Galbraith, R.F., Green, P.F., 1990, Estimating the component ages in a finite mixture: *International Journal of Radiation Applications and Instrumentation. Part D. Nuclear Tracks and Radiation Measurements*, 17(3), 197-206.

Garduño-Martínez, D.E., Puig, T.P., Solé, J., Martini, M., Alcalá-Martínez, J.R., 2015, K-Ar illite-mica age constraints on the formation and reactivation history of the El Doctor fault zone, central Mexico: *Revista Mexicana de Ciencias Geológicas*, 32(2), 306-322.

Gleadow, A.J.W., Duddy, I.R., Green, P.F., Lovering, J.F., 1986, Confined fission track lengths in apatite: a diagnostic tool for thermal history analysis: *Contributions to Mineralogy and Petrology*, 94(4), 405-415.

Godínez-Urban, A., Lawton, T.F., Garza, R.S.M., Iriondo, A., Weber, B., López-Martínez, M., 2011, Jurassic volcanic and sedimentary rocks of the La Silla and Todos Santos Formations, Chiapas: Record of Nazas arc magmatism and rift-basin formation prior to opening of the Gulf of Mexico: *Geosphere*, 7(1), 121-144.

Goldoff, B., Webster, J.D., Harlov, D.E., 2012, Characterization of fluorochlorapatites by electron probe microanalysis with a focus on time-dependent intensity variation of halogens: *American Mineralogist*, 97(7), 1103-1115.

González-Guzmán, R., Weber, B., Manjarrez-Juárez, R., Cisneros de León, A., Hecht, L., Herguera-García, J.C., 2016, Provenance, age constraints and metamorphism of Ediacaran metasedimentary rocks from the El Triunfo Complex (SE Chiapas, México): evidence for Rodinia breakup and Iapetus active margin: *International Geology Review*, 58(16), 2065-2091.

Green, P.F., 1985, Comparison of zeta calibration baselines for fission-track dating of apatite, zircon and sphene: *Chemical Geology: Isotope Geoscience section*, 58(1-2), 1-22.

Green, P.F., Duddy, I.R., Laslett, G.M., Hegarty, K.A., Gleadow, A.W., Lovering, J.F., 1989, Thermal annealing of fission tracks in apatite 4. Quantitative modelling techniques and extension to geological timescales: *Chemical Geology: Isotope Geoscience Section*, 79(2), 155-182.

Gutiérrez-Gil, R., 1956, Bosquejo geológico del Estado de Chiapas, in *20th International Geological Congress*, México, D.F., Excursión C-15, incl., geologic map (9-32).

Guzmán-Speziale, M., 2010, Beyond the Motagua and Polochic faults: Active strike-slip faulting along the western North America-Caribbean plate boundary zone: *Tectonophysics*, 496(1), 17-27.

Guzmán-Speziale, M., Pennington, W.D., Matumoto, T., 1989, The triple junction of the North America, Cocos, and Caribbean plates: Seismicity and tectonics: *Tectonics*, 8(5), 981-997.

Hasebe, N., Arai, S., 2007, LA-ICP-MS-FT dating of age standards: *Fission Track News Letters*, 20, 40-4.

Hasebe, N., Barbarand, J., Jarvis, K., Carter, A., Hurford, A.J., 2004, Apatite fission-track chronometry using laser ablation ICP-MS: *Chemical Geology*, 207(3), 135-145.

Hasebe, N., Carter, A., Hurford, A.J., Arai, S., 2009, The effect of chemical etching on LA-ICP-MS analysis in determining uranium concentration for fission-track chronometry: Geological Society, London, Special Publication 324, 37-46.

Hasebe, N., Tamura, A., Arai, S., 2013, Zeta equivalent fission-track dating using LA-ICP-MS and examples with simultaneous U-Pb dating: *Island Arc*, 22(3), 280-291.

Hurford, A.J., Green, P.F., 1983, The zeta age calibration of fission-track dating: *Chemical Geology*, 41, 285-317.

Jonckheere, R., Van den haute, P., Ratschbacher, L., 2015, Standardless fission-track dating of the Durango apatite age standard: *Chemical Geology*, 417, 44-57.

Ketcham, R.A., 2005, Forward and inverse modeling of low-temperature thermochronometry data: *Reviews in Mineralogy and Geochemistry*, 58(1), 275-314.

Ketcham, R.A., Donelick, R.A., Carlson, W.D., 1999, Variability of apatite fission-track annealing kinetics. III. Extrapolation to geological time scales: *American Mineralogist*, 84, 1235-1255.

Ketcham, R.A., Carter, A., Donelick, R.A., Barbarand, J., Hurford, A.J., 2007, Improved modeling of fission-track annealing in apatite: *American Mineralogist*, 92(5-6), 799-810.

Lesnov, F.P., 2012, Rare Earth Elements in Ultramafic and Mafic Rocks and their Minerals, Minor and accessory minerals: London, UK, Taylor and Francis Group, 314 pp.

Lisker, F., Ventura, B., Glasmacher, U.A., 2009, Apatite thermochronology in modern geology: Geological Society, London, Special Publications, 324(1), 1-23.

Liu, W., Zhang, J., Sun, T., Wang, J., 2014, Application of apatite U-Pb and fission-track double dating to determine the preservation potential of magnetite-apatite deposits in the Luzong and Ningwu volcanic basins, eastern China: *Journal of Geochemical Exploration*, 138, 22-32.

Mandujano-Velásquez, J., 1996, Cuatro megasecuencias de evolución litoestratigráfica en la Sierra de Chiapas: *Boletín de la Asociación Mexicana de Geólogos Petroleros*, 45, 46-60.

Martens, U.C., Brueckner, H.K., Mattinson, C.G., Liou, J.G., Wooden, J.L., 2012, Timing of eclogite-facies metamorphism of the Chuacús complex, Central Guatemala: record of Late Cretaceous continental subduction of North America's sialic basement: *Lithos*, 146, 1-10.

Mark, C., Gupta, S., Carter, A., Mark, D.F., Gautheron, C., Martín, A., 2014, Rift flank uplift at the Gulf of California: No requirement for asthenospheric upwelling: *Geology*, 42(3), 259-262.

Martínez-Amador, H., Rosendo-Brito, B., Fitz-Bravo, C., Tinajera-Fuentes, E., Beltrán-Castillo, H.D., 2005, Carta Geológico-Minera Tuxtla Gutiérrez E5-11, escala 1:250,000: Pachuca, Hidalgo, Servicio Geológico Mexicano, 1 map.

Martini, M., Ortega-Gutiérrez, F., 2016, Tectono-stratigraphic evolution of eastern Mexico during the break-up of Pangea: A review: *Earth-Science Reviews*, doi:10.1016/j.earscirev.2017.06.013.

Martini, M., Ramírez-Calderón, M., Solari, L., Villanueva-Amadoz, U., Zepeda-Martínez, M., Ortega-Gutiérrez, F., Elías-Herrera, M., 2016, Provenance analysis of Jurassic sandstones from the Otlaltepec Basin, southern Mexico: Implications for the reconstruction of Pangea breakup: *Geosphere*, GES01366-1.

McDowell, F.W., McIntosh, W.C., Farley, K.A., 2005, A precise $^{40}\text{Ar}/^{39}\text{Ar}$ reference age for the Durango apatite (U-Th)/He and fission-track dating standard: *Chemical Geology*, 214, 249-263.

Meneses-Rocha, J.J., 1985, Tectonic evolution of the Strike-slip Fault province of Chiapas, Mexico: Austin, University of Texas at Austin, M. Sc. Thesis, 315 pp.

Meneses-Rocha, J.J., 1991, Tectonic development of the Ixtapa graben, Chiapas, Mexico: Austin, University of Texas at Austin, Ph. D. Thesis, 308 pp.

Meneses-Rocha, J.J., 2001, Tectonic evolution of the Ixtapa Graben, an example of a strike-slip basin of southeastern Mexico: Implications for regional petroleum systems, in Bartolini, C., Buffler, R.T., Cantú-Chapa, A. (eds.), The western Gulf of Mexico basin: Tectonics, sedimentary basins and petroleum systems: American Association of Petroleum Geologists Memoir, 75, 183-216.

Michalzik, D., 1991, Facies sequence of Triassic-Jurassic red beds in the Sierra Madre Oriental (NE Mexico) and its relation to the early opening of the Gulf of Mexico: *Sedimentary Geology*, 71(3-4), 243-259.

Molina-Garza, R.S., Geissman, J.W., Wawrzyniec, T.F., Peña Alonso, T.A., Iriondo, A., Weber, B., Aranda-Gómez, J., 2015, Geology of the coastal Chiapas (Mexico) Miocene plutons and the Tonalá shear zone: Syntectonic emplacement and rapid exhumation during sinistral transpression: *Lithosphere*, 7, 257-274.

Morán-Zenteno, D.J., Keppie, D.J., Martiny, B., González-Torres, E., 2009, Reassessment of the Paleogene position of the Chortís block relative to southern Mexico: Hierarchical ranking of data and features: *Revista Mexicana de Ciencias Geológicas*, 26(1), 177-188.

Moravec, D., 1983, Study of the Concordia Fault System near Jericó, Chiapas, Mexico: Austin, University of Texas at Austin, M. Sc. Thesis, 155 pp.

Ortega-Obregón, C., Solari, L., Abdullin, F., 2016, Towards the understanding of the cooling history of a magmatic body: U-Pb ages of zircon and apatite from the Chiapas Batholith, Mexico, using LA-ICPMS, in 10th South American Symposium on Isotope Geology (SSAGI): Puerto Vallarta, México, p. 150.

Padilla y Sánchez, R.J., 2007, Evolución geológica del sureste mexicano desde el Mesozoico al presente en el contexto regional del Golfo de México: *Boletín de la Sociedad Geológica Mexicana*, 59, 19-42.

Paton, C., Hellstrom, J., Paul, B., Woodhead, J., Hergt, J., 2011, Iolite: Freeware for the visualisation and processing of mass spectrometric data: *Journal of Analytical Atomic Spectrometry*, 26(12), 2508-2518.

Pearce, N.J., Perkins, W.T., Westgate, J.A., Gorton, M.P., Jackson, S.E., Neal, C.R., Chinery, S.P., 1997, A compilation of new and published major and trace element data for NIST SRM 610 and NIST SRM 612 glass reference materials: *Geostandards and Geoanalytical Research*, 21(1), 115-144.

Pedrazzini, C., Holguín, N., Moreno, R., 1982, Evolución Geológica-Geoquímica de la parte noroccidental del Golfo de Tehuantepec: Instituto Mexicano del Petróleo Revista, 14, 6-26.

Pérez-Gutiérrez, R., Solari, L.A., Gómez-Tuena, A., Valencia, V.A., 2009, El terreno Cuicateco: ¿cuencia oceánica con influencia de subducción del Cretácico Superior en el sur de México? Nuevos datos estructurales, geoquímicos y geocronológicos: *Revista Mexicana de Ciencias Geológicas*, 26(1), 222-242.

Pindell, J., Kennan, L., Draper, G., Maresch, W.V., Stanek, K.P., 2006, Foundations of Gulf of Mexico and Caribbean evolution: Eight controversies resolved: *Geologica Acta*, 4, 303-341.

Pompa-Mera, V., 2009, Geoquímica y Geocronología de los Complejos Intrusivos en el sureste de Chiapas, México: México, Universidad Nacional Autónoma de México, M. Sc. Thesis, 160 pp.

Quetzada-Muñetón, J.M., 1983, Las Formaciones San Ricardo y Jericó del Jurásico Medio-Cretácico Inferior en el SE de México: *Boletín de la Asociación Mexicana de Geólogos Petroleros*, 35, 37-64.

Quetzada-Muñetón, J.M., 1987, El Cretácico medio-Superior y el límite Cretácico Superior-Terciario inferior en la Sierra de Chiapas: *Boletín de la Asociación Mexicana de Geólogos Petroleros*, 39, 3-98.

Ratschbacher, L., Franz, L., Min, M., Bachmann, R., Martens, U., Stanek, K., Stübner, K., Nelson, B.K., Herrmann, U., Weber, B., López-Martínez, M., Jonckheere, R., Sperner, B., Tichomirowa, M., McWilliams, M.O., Gordon, M., Meschede, M., and Bock, P., 2009, The North American-Caribbean plate boundary in Mexico-Guatemala-Honduras, in James, K., Lorente, M., Pindell, J. (eds.), The origin and evolution of the Caribbean plate: Geological Society of London, Special Publications, 328, 219-293.

Reiners, P.W., Brandon, M.T., 2006, Using thermochronology to understand orogenic erosion: *Annual Review of Earth and Planetary Sciences*, 34, 419-466.

Reiners, P.W., Ehlers, T.A., Zeitler, P.K., 2005, Past, present, and future of thermochronology: *Reviews in Mineralogy and Geochemistry*, 58(1), 1-18.

Rosales-Domínguez, M.D.C., 1998, Biohorizontes cronoestratigráficos en las facies carbonatadas de plataforma del Cretácico medio-superior de Chiapas, México: *Revista Mexicana de Ciencias Geológicas*, 15(1), 73-77.

Rosales-Domínguez, M.D.C., Bermúdez-Santana, J.C., Aguilar-Piña, M., 1997, Mid and Upper Cretaceous foraminiferal assemblages from the Sierra de Chiapas, southeastern Mexico: *Cretaceous Research*, 18, 697-712.

Rubio-Cisneros, I.I., Lawton, T.F., 2011, Detrital zircon U-Pb ages of sandstones in continental red beds at Valle de Huizachal, Tamaulipas, NE Mexico: Record of Early-Middle Jurassic arc volcanism and transition to crustal extension: *Geosphere*, 7(1), 159-170.

Salvador, A., 1987, Late Triassic–Jurassic paleogeography and origin of Gulf of Mexico basin: American Association of Petroleum Geologists Bulletin, 71, 419–451.

Sánchez, M.O., Franco, N.A., Navarrete, S.F., Martínez, M.G., 2004, Estratigrafía y evolución de facies del Cretácico Superior en el Sureste de México: Boletín de la Asociación Mexicana de Geólogos Petroleros, Special Paper No. 697, 39–61.

Sánchez-Barreda, L.A., 1981, Geologic evolution of the continental margin of the Gulf of Tehuantepec in southwestern Mexico: Austin, University of Texas at Austin, Ph.D. Thesis, 191 pp.

Sánchez-Montes de Oca, R., 1979, Geología petrolera de la Sierra de Chiapas: Boletín de la Asociación Mexicana de Geólogos Petroleros, 31, 67–97.

Sánchez-Montes de Oca, R., 2006, Curso Cuenca del Sureste: México, Petróleos Mexicanos, 296 pp.

Schaaf, P., Morán-Zenteno, D., Hernández-Bernal, M.D.S., Solís-Pichardo, G., Tolson, G., Köhler, H., 1995, Paleogene continental margin truncation in southwestern Mexico: Geochronological evidence: Tectonics, 14(6), 1339–1350.

Schaaf, P., Weber, B., Weis, P., Grob, A., Ortega-Gutiérrez, F., Kohler, H., 2002, The Chiapas Massif (Mexico) revised: New geologic and isotopic data and basement characteristics, in Miller, H.E. (ed.), Contributions to Latin-American Geology: Neues Jahrbuch für Geologie und Paläontologie, Abhandlungen, 225, 1–23.

Solari, L.A., García-Casco, A., Martens, U., Lee, J.K., Ortega-Rivera, A., 2013, Late Cretaceous subduction of the continental basement of the Maya block (Rabinal Granite, central Guatemala): Tectonic implications for the geodynamic evolution of Central America: Geological Society of America Bulletin, 125(3–4), 625–639.

Solé, J., Pi, T., 2005, An empirical calibration for ${}^4\text{He}$ quantification in minerals and rocks by laser fusion and noble gas mass spectrometry using Cerro de Mercado (Durango, Mexico) fluorapatite as a standard: Analytica Chimica Acta, 535, 325–330.

Steiner, M.B., 2005, Pangean reconstruction of the Yucatan Block: Its Permian, Triassic, and Jurassic geologic and tectonic history: Geological Society of America Special Papers, 393, 457–480.

Svojtka, M., Košler, M., 2002, Fission-track dating of zircon by LA-ICP-MS, in 12th Annual V. M. Goldschmidt Conference, Davos, Switzerland: Journal of Conference Abstracts, Special Supplement of Geochimica et Cosmochimica Acta, 66, A756.

Thomson, S.N., Gehrels, G.E., Ruiz, J., Buchwaldt, R., 2012, Routine low-damage apatite U–Pb dating using laser ablation–multicollector-ICPMS: Geochemistry, Geophysics, Geosystems, 13(2), DOI:10.1029/2011GC003928.

Torres, R., Ruiz, J., Patchett, P.J., Grajales, J.M., 1999, Permo-Triassic continental arc in eastern Mexico: Tectonic implications for reconstructions of southern North America: Geological Society of America, Special Paper, 340, 191–196.

Torres-de León, R., Solari, L.A., Ortega-Gutiérrez, F., Martens, U., 2012, The Chortís Block–Southwestern México connections: U–Pb zircon geochronology constraints: American Journal of Science, 312(3) 288–313.

Vermeesch, P., 2009, RadialPlotter: A Java application for fission track, luminescence and other radial plots: Radiation Measurements, 44, 409–410.

Vermeesch, P., 2017, Statistics for LA-ICP-MS based fission track dating: Chemical Geology, 456, 19–27.

Vermeesch, P., Miller, D.D., Graham, S.A., De Grave, J., McWilliams, M.O., 2006, Multimethod detrital thermochronology of the Great Valley Group near New Idria, California: Geological Society of America Bulletin, 118, 210–218.

Wagner, G., Van den haute, P., 1992, Fission Track Dating: Dordrecht, Holland, Kluwer, Earth Sciences Library, 285 pp.

Weber, B., Cameron, K.L., Osorio, M., Schaaf, P., 2005, A late Permian tectonothermal event in Grenville crust of the southern Maya terrane: U–Pb zircon ages from the Chiapas Massif, southeastern Mexico: International Geology Review, 47, 509–529.

Weber, B., Schaaf, P., Valencia, V.A., Iriondo, A., Ortega-Gutiérrez, F., 2006, Provenance ages of late Paleozoic sandstones (Santa Rosa Formation) from the Maya Block, SE México: implications on the tectonic evolution of western Pangea: Revista Mexicana de Ciencias Geológicas, 23(3), 262–276.

Weber, B., Iriondo, A., Premo, W.R., Hecht, L., Schaaf, P., 2007, New insights into the history and origin of the southern Maya block, SE México: U–Pb–SHRIMP zircon geochronology from metamorphic rocks of the Chiapas massif: International Journal of Earth Sciences, 96, 253–269.

Weber, B., Valencia, V.A., Schaaf, P., Pompa-Mera, V., Ruiz, J., 2008, Significance of Provenance Ages from the Chiapas Massif Complex (Southeastern Mexico): Redefining the Paleozoic Basement of the Maya Block and Its Evolution in a Peri-Gondwanan Realm: Journal of Geology, 116, 619–639.

Weber, B., Valencia, V.A., Schaaf, P., Ortega-Gutiérrez, F., 2009, Detrital zircon ages from the Lower Santa Rosa Formation, Chiapas: Implications on regional Palaeozoic stratigraphy: Revista Mexicana de Ciencias Geológicas, 26, 260–276.

Witt, C., Brichau, S., Carter, A., 2012, New constraints on the origin of the Sierra Madre de Chiapas (south Mexico) from sediment provenance and apatite thermochronometry: Tectonics, 31(6), doi:10.1029/2012TC003141.

Manuscript received: may 24, 2017

Corrected manuscript received: january 23, 2018

Manuscript accepted: february 16, 2018